Preface

This thesis consists of the work I did over the last two years on effect of spin transition phenomena of signal crystal mineral ferropericlase (Mg0.92,Fe0.08) O up to 89 GPa.

SINGLE-CRYSTAL ELASTICITY OF FERROPERICLASE (MG0.92FE0.08)O TO 89 GPa

by

Xinyue Tong

Thesis

Presented to the Faculty of the Graduate School of
The University of Texas at Austin
in Partial Fulfillment
of the Requirements
for the Degree of

Master of Science in Geological Sciences

The University of Texas at Austin

May 2013

Acknowledgements

At this moment, I would like give my deep appreciation to my supervisor Professor Jung-Fu Lin, for his guide and support, and also for his valuable advice both on my study and my future plan. Secondly, I would like to give equal appreciation to my co-worker Jing Yang. She prepared all the cells that we need and did a lot of analysis on the data. Moreover, she is doing a great job on her part of this project. Without her selfless helps, I could not finish my project this smooth and quick.

Moreover, I would like to give thanks to my officemate Jin Liu and his wife Hailing Gu, and my previous roommate Chang Lu, for treating me like a family and making my life in Austin colorful.

Last but not least, I would like to give thanks to my family. Thanks to my beloved wife Qiaoyun Ma, for her love, understand and support. I would not reach my goal without her. And thanks to my parents for their encouragements and led me my way to Science.

SINGLE-CRYSTAL ELASTICITY OF FERROPERICLASE (MG0.92FE0.08)O TO 89 GPa

Abstract

Xinyue Tong, M.S. Geo. Sci.

The University of Texas at Austin, 2014

Supervisor: Jung-Fu Lin

This study focuses on investigating the effect of the electronic spin transition of iron on elasticity of the candidate lower mantle ferropericlase (Mg,Fe)O, as this may be of relevance to our understanding seismic velocity structures of the Earth's lower mantle. The elastic tensor of $(Mg_{0.92}Fe_{0.08})O$ at HS state, LS state, and through the pressure-induced HS-to-LS transition has been measure by use both BLS and ISS. There is a large pressure range which c_{11} and c_{12} exhibit a softening, while c_{44} does not register such anomaly. Compare with previously published data of ferropericlase with close compositions ([*Marquardt et al.*, 2009b], BLS measurement of $(Mg_{0.9}Fe_{0.1})O$ and [*Crowhurst et al.*, 2008], ISS measurement of $(Mg_{0.94}Fe_{0.06})O$), similar but even more pronounced behavior of elastic properties has been measured in this study by taking the advantage of simultaneity measurement on BLS and ISS. Current theoretical and experimental studies [*Sturhahn et al.*, 2005, *Tsuchiya et al.*, 2006, *Lin et al.*, 2007] indicate that the spin transition take place over an extended range of depth along the expected geotherm, which abrupt changes in compressional and bulk sound velocity are not expected.

Figure

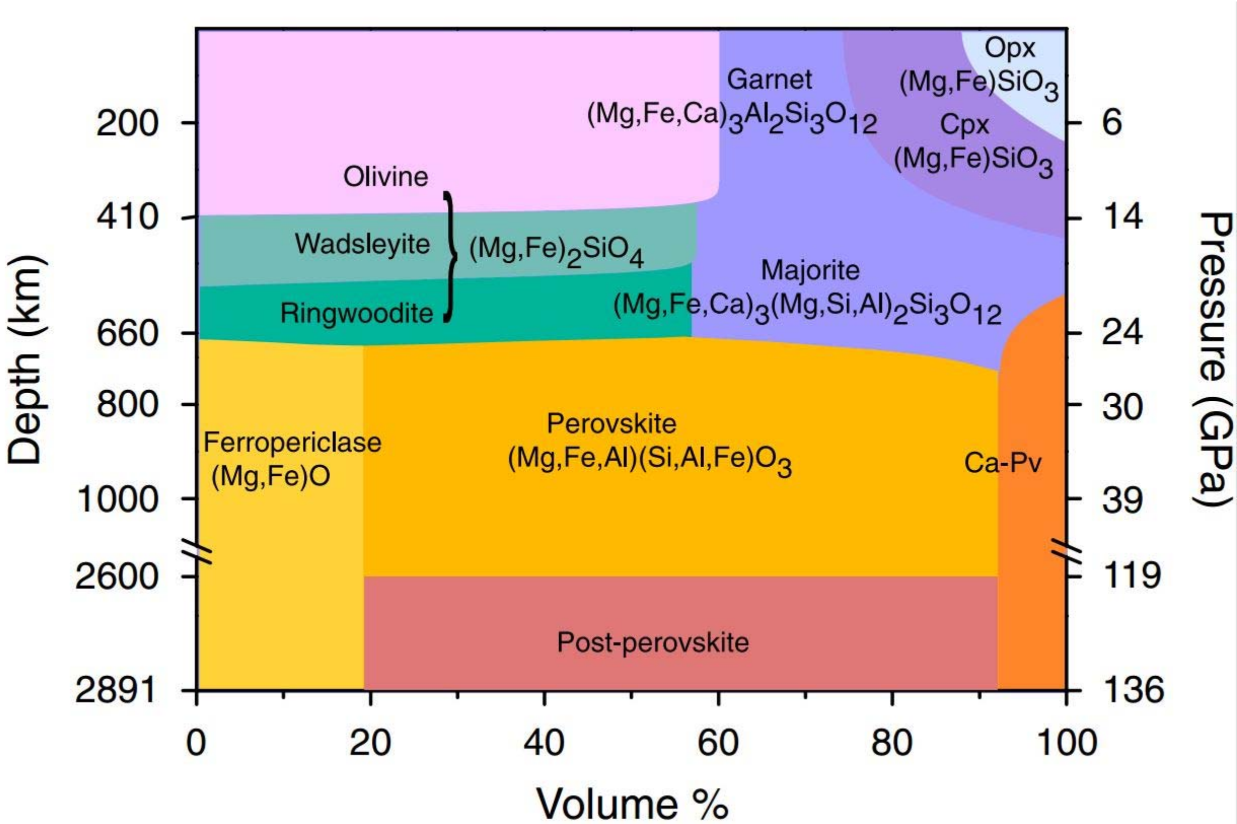

Figure 1.1 Mineralogical model of the Earth's interior as a function of depth (pressure)[Lin et al., 2013]. Mineral abbreviation: Opx and cpx, orthopyroxene and clinopyroxene, respectively; CaPv, calcium silicate perovskite.

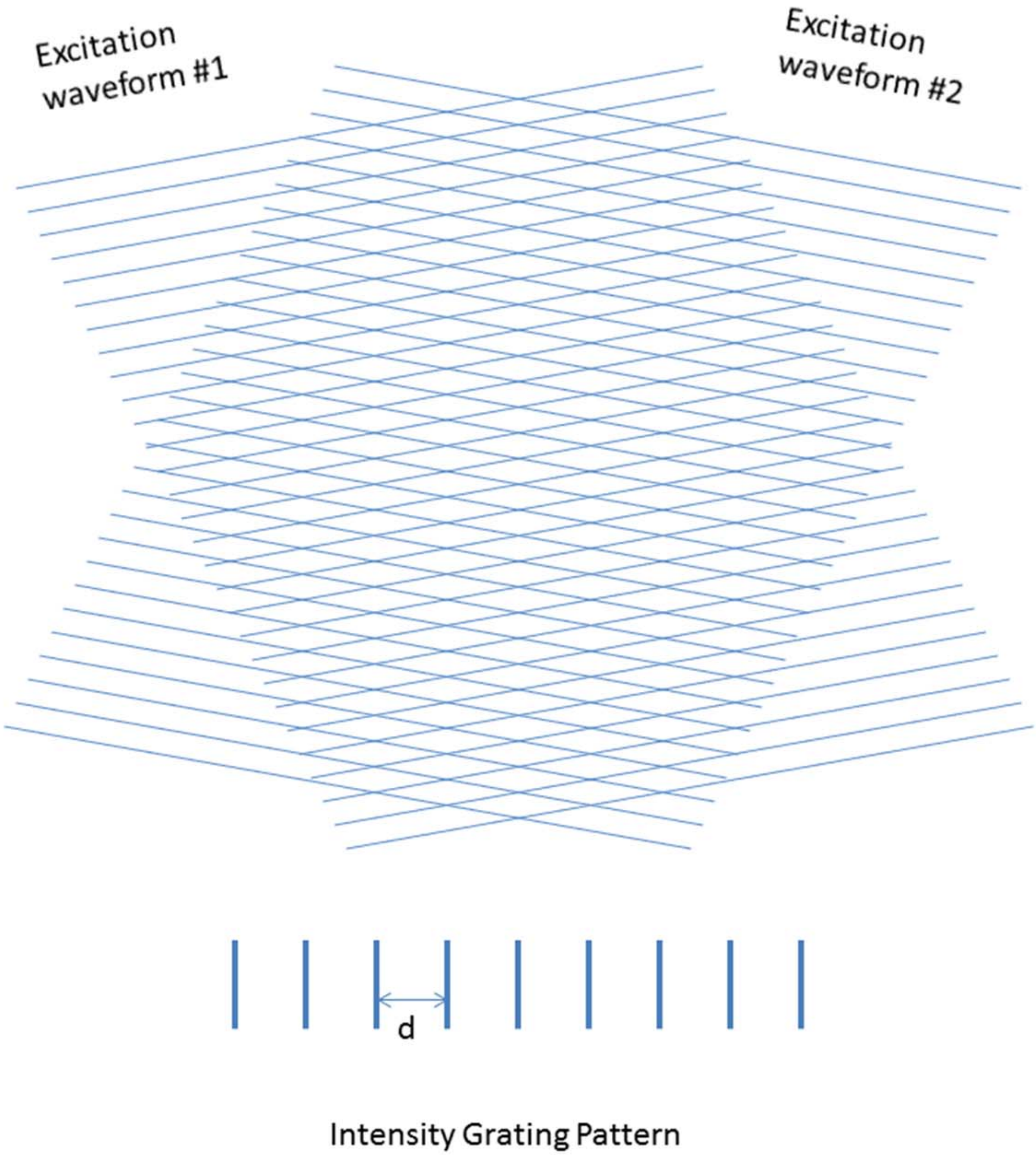

Figure 2.1 Formation of the interference grating pattern by crossing two excitation pulses.

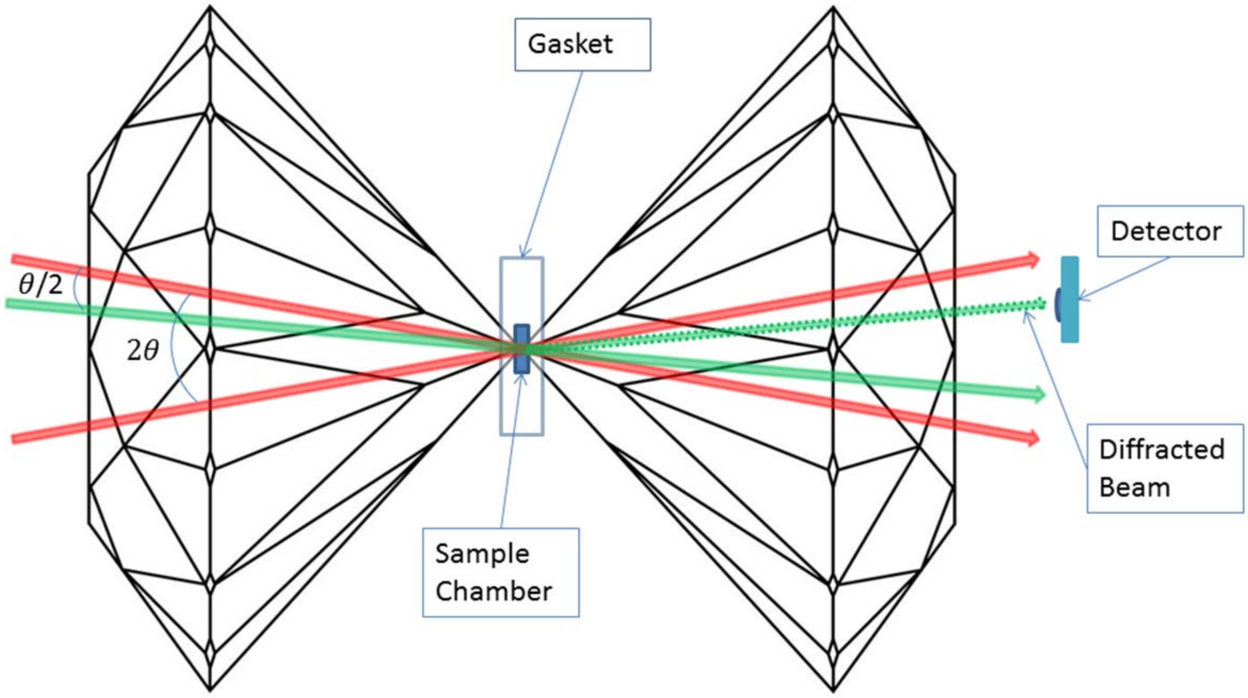

Figure 2.2 Diamond Anvil Cell, pump (Red) and probe (Green) beams geometry.

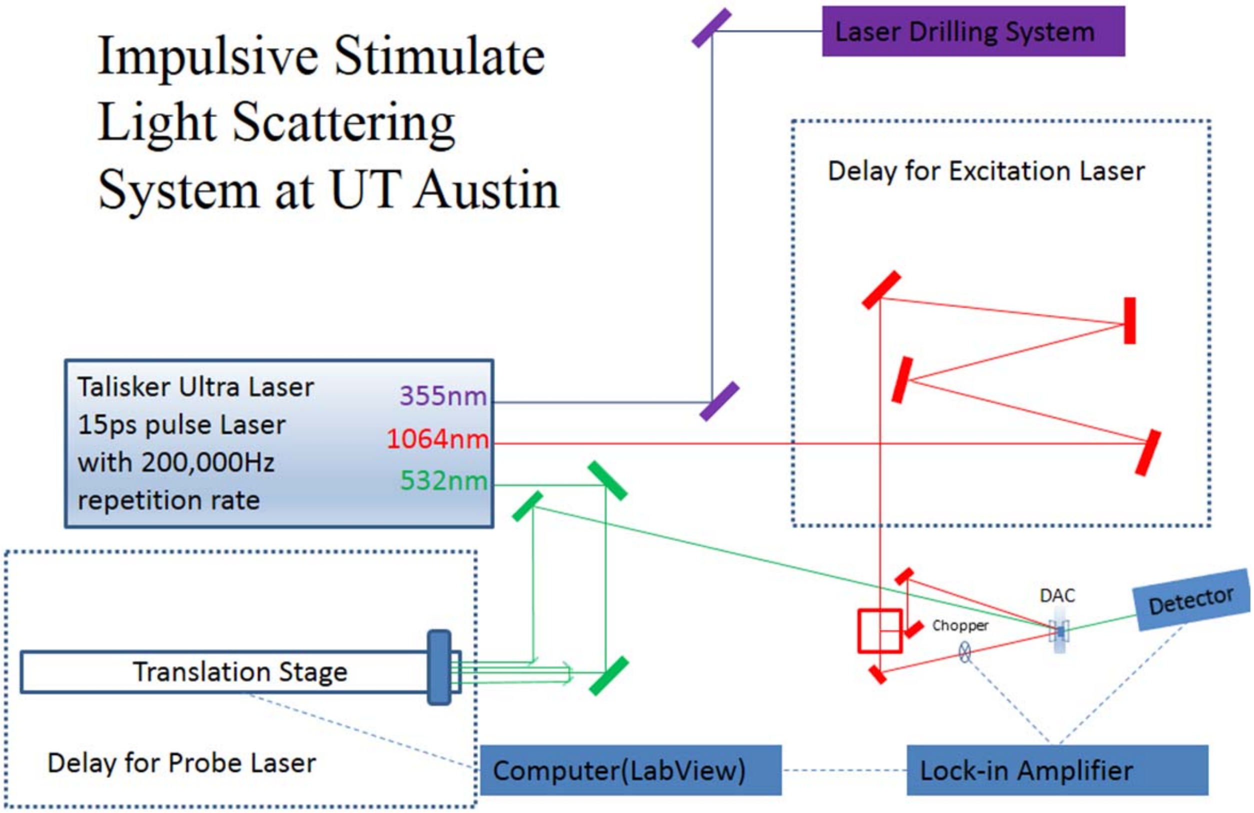

Figure 2.3 Schematic of the Impulsive Stimulated Light Scattering setup in the Mineral Physics Lab at The University of Texas at Austin. It is equipped with a Coherent Talisker Ultra Laser system, a PD Detector, a Lock-in Amplifier, a translational stage for elasticity measurements, and a computer to control the whole system through LabView.

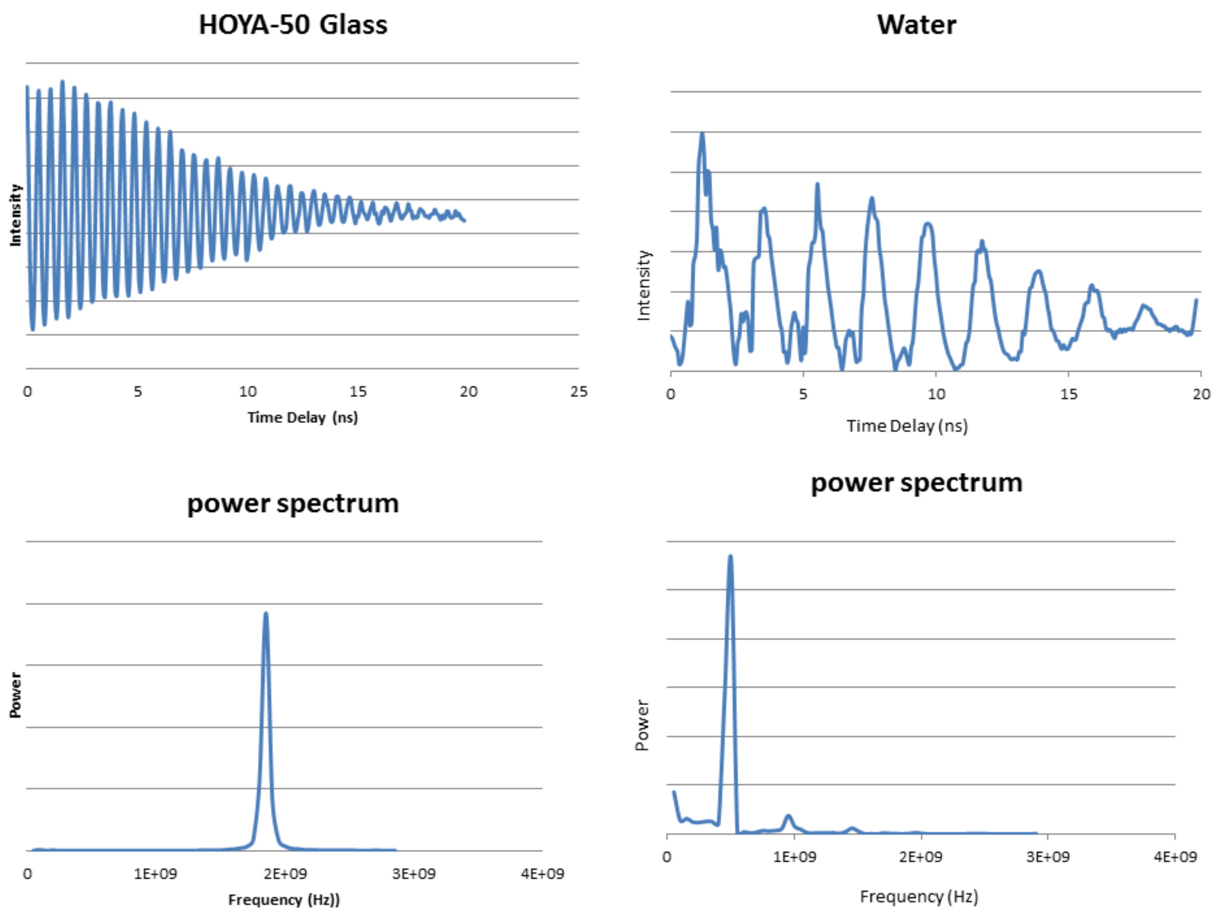

Figure 2.4 ***Left***, Glass ISS measurement in time domain and its power spectrum in frequency domain; ***Right***, Water ISS measurement in time domain and their power spectrum in frequency domain. Those are used for ISS calibration purpose.

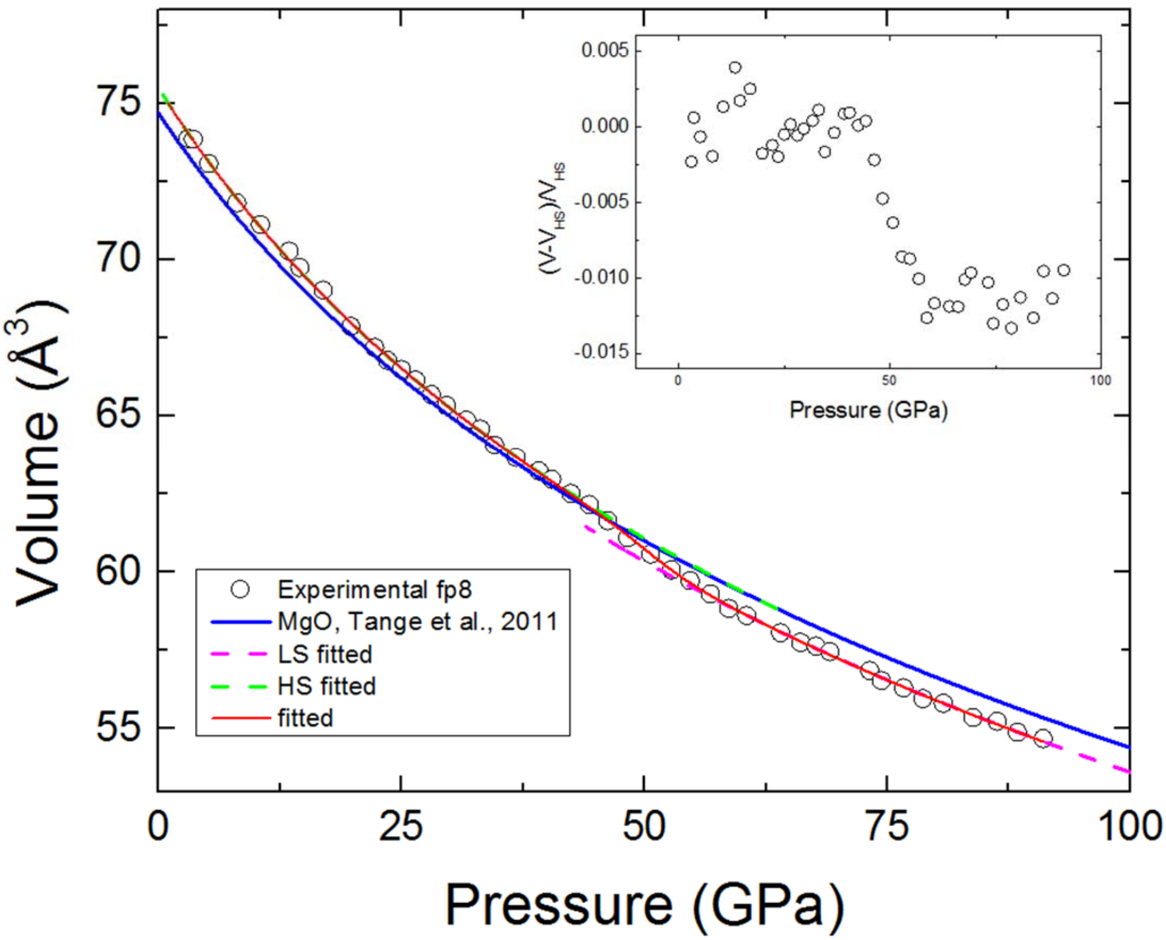

Figure 4.1 Isothermal compression curve of ($Mg_{0.92}Fe_{0.08}$)O. The green and pink dished lines represent the extrapolation of the HS and LS phase. The blue solid line show results for MgO (Tange et al., 2009) for comparison. The inset in the upper right corner shows the pressure dependent ratio of unit cell volume changes and HS unit cell volume; the anomalous in spin crossover and LS are clearly visible.

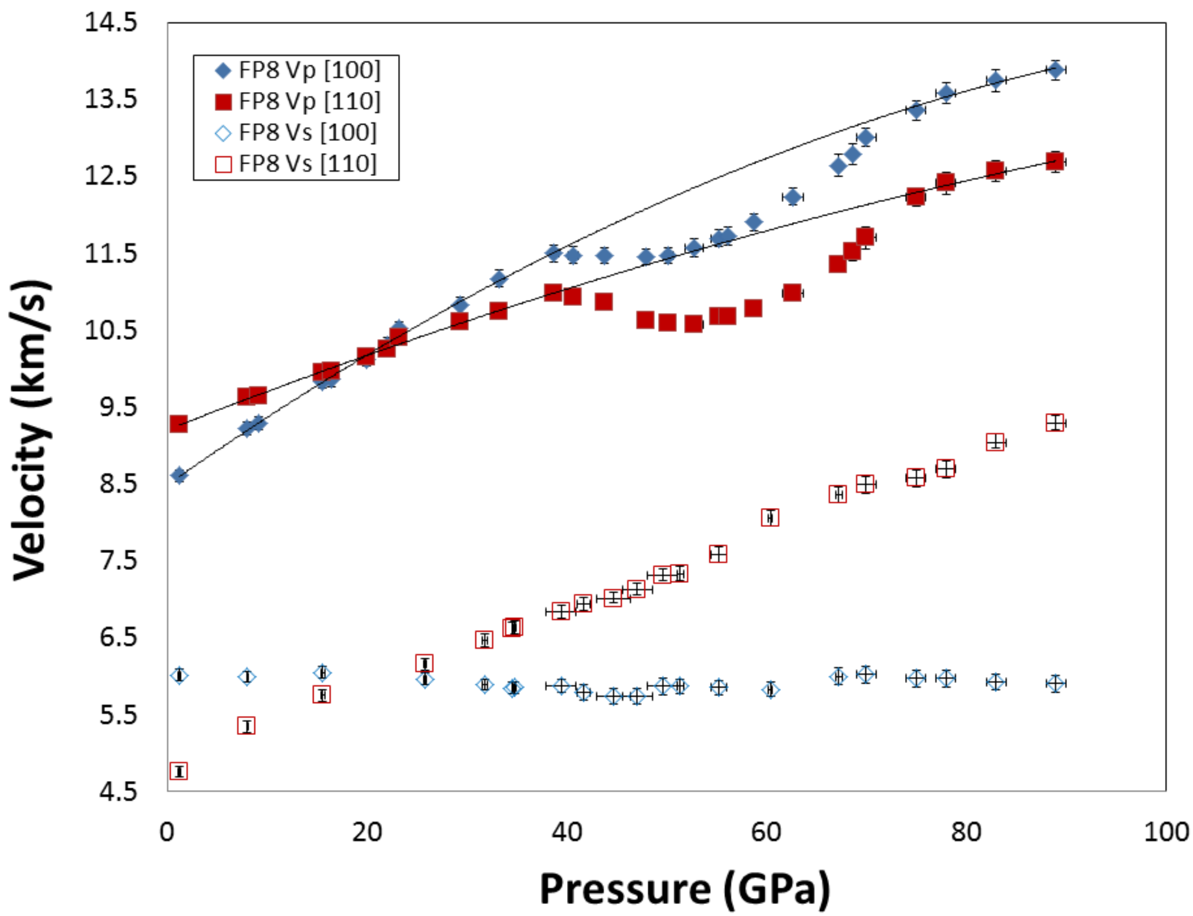

Figure 4.6 Acoustic wave velocity as function of pressure for propagation in the (100) plane of single crystal ($Mg_{0.92}Fe_{0.08}$)O. Solid-filled diamond and square are compressional wave velocity along [100] and [110] principle axis acquired by Impulsive Stimulated Scattering. Non-filled diamond and square are Brillouin Scattering measurements of share wave velocity.

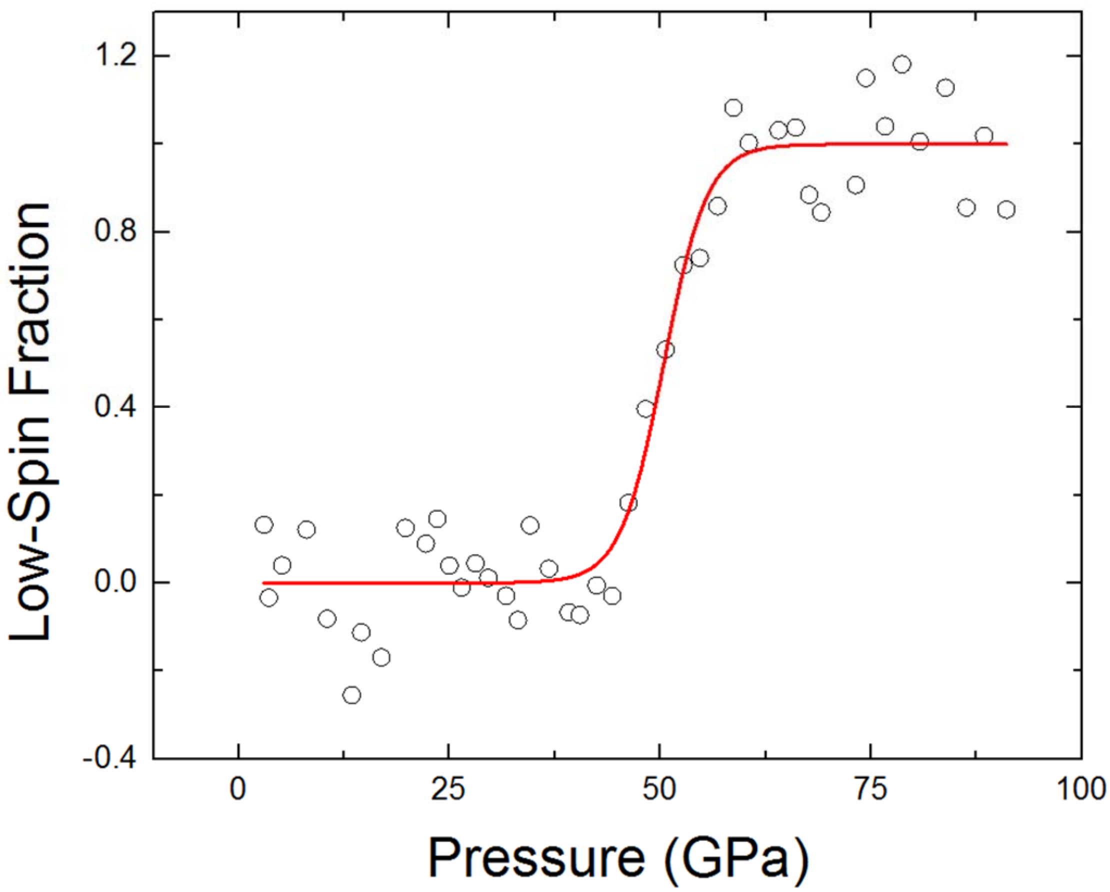

Figure 4.2 Derived low spin fraction of ferropericlase as a function of pressure compared with the fitting result. Open circles are experimental measurements at room temperature (300 K) and the red line is the fitting result.

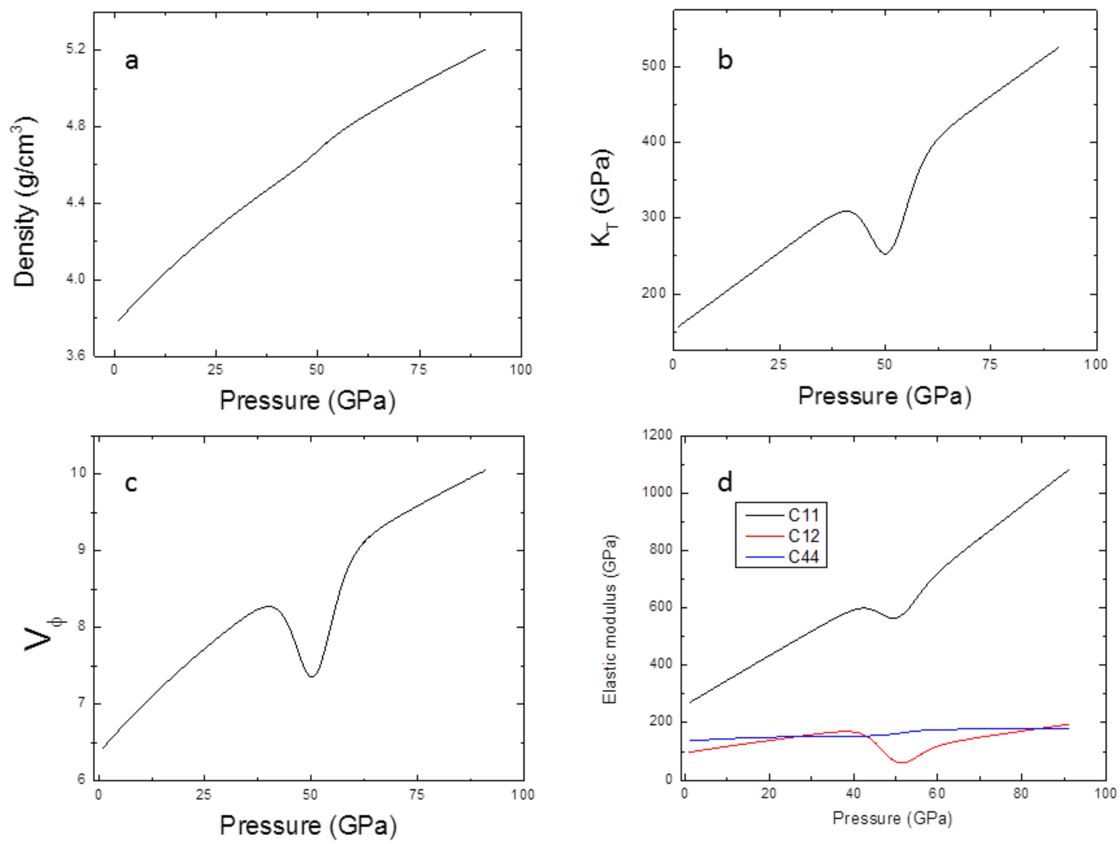

Figure 4.3 Density (a), isothermal bulk module (b), and bulk sound velocity(c) of single crystal ($Mg_{0.92}Fe_{0.08}$)O modeled [Wentzovich et al., 2009] from X-ray diffraction measurement. Elastic modulus of single crystal ($Mg_{0.92}Fe_{0.08}$)O modeled [Wu et al., 2013 and Birch 1978] from BLS and ISS measurements (d).

Wait from Jill

Figure 4.5 The representative Brillouin spectra along [100] (left) and [110] (right) at 55GPa.

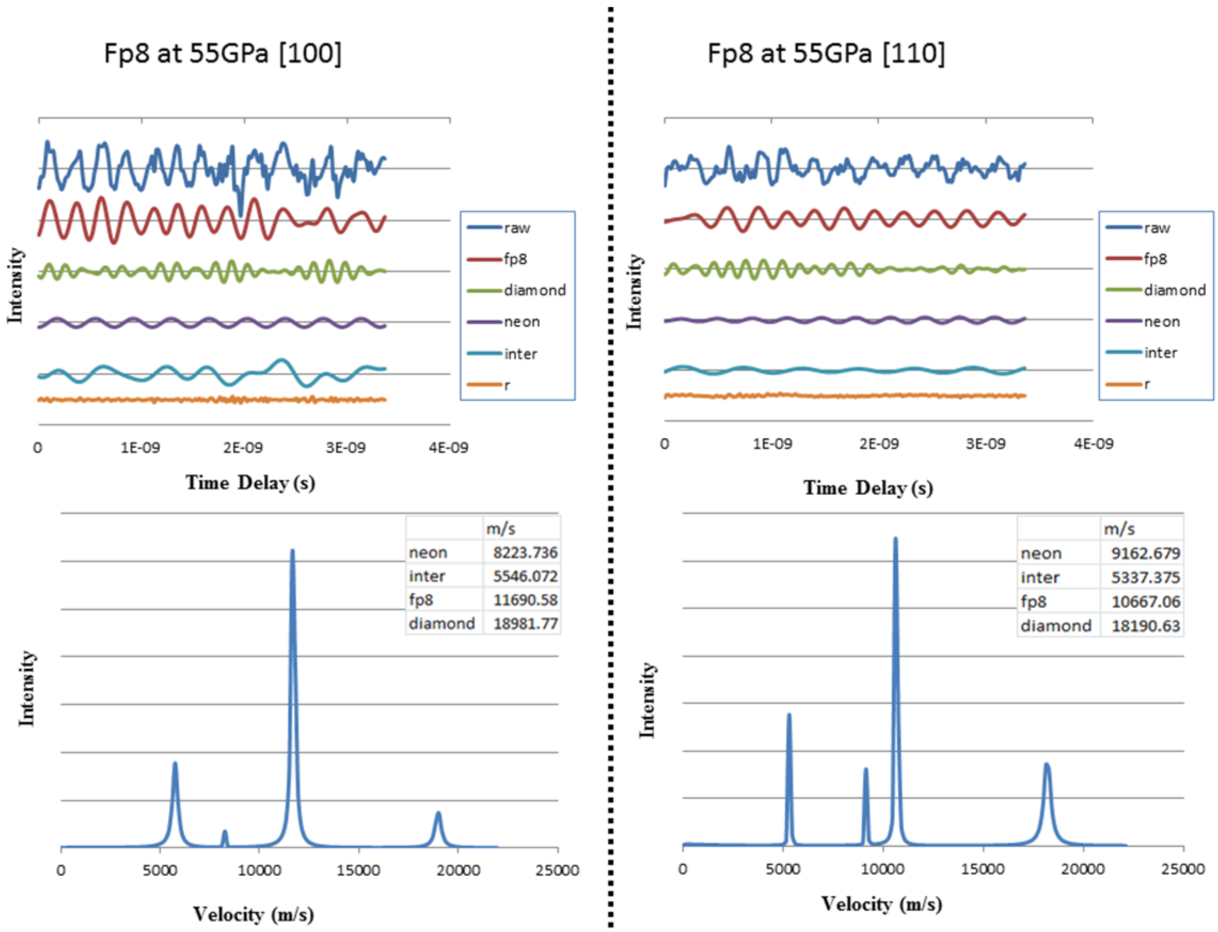

Figure 4.5 The representative ISS spectra along [100] (left) and [110] (right) at 55GPa. **Top**, consist of original time delay measurements (raw), filtered signals for Fp8(Vp), Diamond (Vp), Neon (pressure medium, Vp), and Interfacial wave velocity, as well as the noise (r). **Bottom**, power spectra of each (Fp8, Diamond, Neon, and Interfacial) interested subject's velocity information

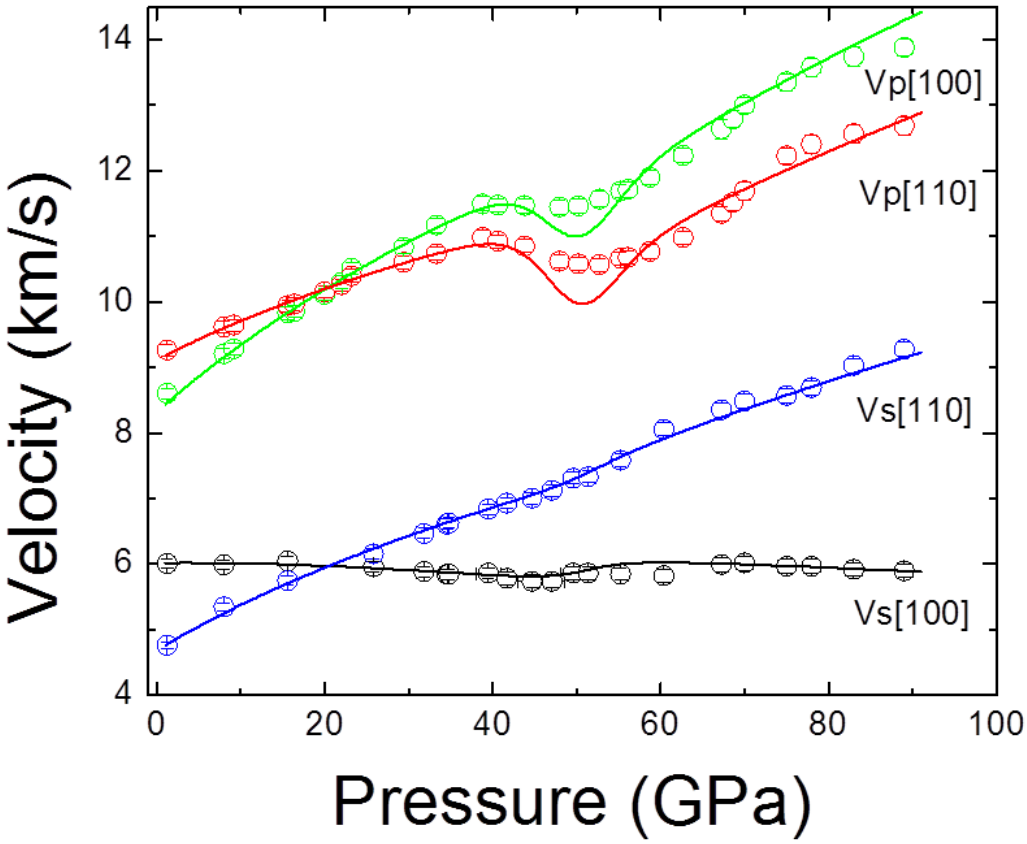

Figure 5.1 Open circles are Vp and Vs measurements from ISS and BLS. Solid lines are predicted velocities profiles by using finite strain theory with the assumption of the spin transition only has a spontaneous strain effect on materials' elastic behaviors. The miss fit (especially within and right after the spin-transition region) between the measured and the predicted velocity profiles indicate that the susceptibility of structural feature Q and the strength of coupling between the Q and the volume stain have to be taken into account for better explain the softening in the spin transition region and the post spin transition relaxation behavior.

P(GPa)	V($\dot{A}^3$)	P(GPa)	V($\dot{A}^3$)	P(GPa)	V($\dot{A}^3$)	P(GPa)	V($\dot{A}^3$)
3.04	73.89±0.13	25.01	66.50±0.04	44.34	62.16±0.12	67.66	57.64±0.11
3.58	73.87±0.03	26.47	66.16±0.01	46.24	61.64±0.02	69.10	57.46±0.15
5.18	73.09±0.04	28.08	65.70±0.04	48.29	61.10±0.09	73.20	56.85±0.09
8.06	71.83±0.12	29.63	65.34±0.01	50.65	60.58±0.01	74.40	56.54±0.15
10.5	71.14±0.08	31.72	64.87±0.03	52.78	59.73±0.10	76.69	56.31±0.04
13.43	70.29±0.26	33.14	64.58±0.09	54.72	59.31±0.06	78.67	55.96±0.18
14.54	69.76±0.11	34.59	64.08±0.13	56.80	58.84±0.12	80.78	55.81±0.01
16.94	69.04±0.17	36.81	63.67±0.03	58.70	58.61±0.02	83.84	55.36±0.13
19.80	67.87±0.13	39.16	63.24±0.08	60.53	58.07±0.04	86.31	55.23±0.14
22.24	67.20±0.09	40.49	62.97±0.09	64.02	57.76±0.04	88.40	54.88±0.02
23.56	66.79±0.15	42.45	62.52±0.05	66.09	57.64±0.11	91.05	54.68±0.15

Table 1 Unit cell volume of $(Mg_{0.94}Fe_{0.06})O$ as function of pressure with uncertainties.

	$c_{11}{}^0$(GPa)	$c_{11}{}'$(GPa)	$c_{12}{}^0$(GPa)	$c_{12}{}'$(GPa)	$c_{44}{}^0$(GPa)	$c_{44}{}'$(GPa)
High-spin phase (0-40 GPa)	260.67 ± 13.03	8.896 ± 0.445	95.40 ± 4.67	2.288 ± 0.114	134.75 ± 6.73	1.010 ± 0.051
Low-spin phase (60-89 GPa)	100.69 ± 5.03	9.860 ± 0.493	5.832 ± 0.292	1.910 ± 0.095	50.54 ± 2.53	2.007 ± 0.100

Table 2 Best fit of Eulerian finite strain equation parameter of $(Mg_{0.94}Fe_{0.06})O$ based on BLS and ISS results.